Healthy and Scar Myocardial Tissue Classification in DE-MRI

Xènia Albà[1,2], Rosa M. Figueras i Ventura[1,2], Karim Lekadir[1,2], and Alejandro F. Frangi[1,2,3,⋆]

[1] Center for Computational Imaging & Simulation Technologies in Biomedicine (CISTIB), Universitat Pompeu Fabra, Barcelona, Spain
[2] Networking Center on Biomedical Research (CIBER-BBN), Barcelona, Spain
[3] Department of Mechanical Engineering, University of Sheffield, Sheffield, UK

Abstract. We propose an automatic technique to segment scar and classify the myocardial tissue of the left ventricle from Delay Enhancement (DE) MRI. The method uses multiple region growing with two types of regions and automatic seed initialization. The region growing criteria is based on intensity distance and the seed initialization is based on a thresholding technique. We refine the obtained segmentation with some morphological operators and geometrical constraints to further define the infarcted area. Thanks to the use of two types of regions when performing the region growing, we are able to segment and classify the healthy and pathological tissues. We have also a third type of tissue in our classification, which includes tissue areas that deserve special attention from medical experts: border-zone tissue or myocardial segmentation errors.

1 Introduction

Magnetic Resonance Imaging (MRI) plays an important role for the assessment of cardiac viability [1]. To this end, Delay Enhancement MRI (DE-MRI) has established itself as a standard imaging protocol in clinical practice to localize and quantify myocardial scar tissue [2]. Due to the large amount of information and in order to remove operator bias, user interaction needs to be reduced or eliminated where possible.

The purpose of our work is to automatically locate the infarcted tissue inside the left ventricle in short axis DE-MRI. First, the left ventricle borders need to be segmented. Following this, tissues inside the myocardium have to be classified.

The first step, segmentation of the myocardium, can be solved in different ways: registering CINE segmentations to DE images [3, 4] or trying to directly segment DE-MRI. The first approach benefits from higher contrast in CINE,

⋆ This research has been partially funded by the Industrial and Technological Development Center (CDTI) under the CENIT-cvREMOD program, by the European Commission's project euHeart (FP7-ICT-224495) and by the Spanish Ministry of Science and Innovation (TIN2011-28067). Alejandro F. Frangi is partially funded by the ICREA-Academia programme.

O. Camara et al. (Eds.): STACOM 2012, LNCS 7746, pp. 62–70, 2013.

but introduces segmentation errors due to slice misalignment and inconsistency in the number of slices. The second one if performed with the right priors can solve these inconsistencies and correct slice misalignments [5].

Once the myocardium contours have been obtained, the scar has to be located. The theory behind the delay enhancement analysis is that the image intensity of the scar is significantly higher than that of healthy myocardial tissue. However, the detection and quantification of the pathological tissues is a difficult task and several issues have to be solved. The contrast between the different tissues is related to the acquisition system and time, which are not always optimal. Moreover, depending on the pathology, the shape and extension of pathological areas, their location with respect to myocardium contours and the keenness of their borders diverge a lot. All this factors make the segmentation difficult and prone to intra and inter-observer variability. Considering this, the development of an automated segmentation of the infarct extent is needed.

Based on the theory behind the DE-MRI, an intuitive method for the detection of the scar is the application of a threshold two or three standard deviations above the average intensity value of a healthy myocardial region [2, 6], or using other metrics [7, 8]. Another approach is to apply clusters [9], or classify myocardial tissue using a support vector machine [3, 10]. The main disadvantage of these methods is the absence of spatial information. Hsu et al. [11] perform a feature analysis after the initial thresholding studying the 3-D connectivity to remove false positive segmentations. In [12], the authors combine both intensity thresholding and spatial information. To avoid the choice of a threshold, the fuzzy c-means algorithm, which provide a membership degree to the class of enhanced pixels, can be applied to the pixels only inside the myocardium [9] or both myocardium and blood pool [13]. Moreover, [14] proposed an algorithm that combines a histogram analysis with a constrained watershed segmentation as part of a combined analysis of coronary arteries, myocardial perfusion, and delay enhancement based on MRI. Elagouni *et al.* [15] use fuzzy thresholding followed by region analysis. In [16], the pathological tissue in the myocardium wall is identified using a MAP-based classifier based on the visual appearance and spatial interaction of the LV pathological tissue as well as healthy tissue.

We propose an automatic technique to classify the myocardial tissues of the left ventricle from DE-MRI. Our method uses a region growing algorithm based on intensity distance with automatic seed selection to segment the healthy tissue, the scar and a third type of tissue (which for most patients is ischemic viable tissue or border-zone tissue). To define the final infarcted area, a post-processing is applied based on morphological operators and location constraints.

The data used in the paper is provided by the STACOM-DEMRI Challenge. The challenge dataset consists of 30 DE-MRI datasets for segmentation of enhanced regions from post-myocardial infarction patients (15) and pigs (15) that have suffered from myocardial ischaemia. The dataset includes the myocardial segmentations and, of each of these 15 datasets, 5 are provided as training samples with manual annotations of the scar.

2 Methodology

Assuming that the myocardium contours have already been obtained, our scar segmentation method consists of five steps, as illustrated in Fig. 1. The automated algorithm selects seeds based on the intensity, and defines a region growing algorithm to, finally, segment the healthy tissue, the scar and a third type of tissue, which would include border-zone tissue and/or myocardial segmentation errors. We have also used some geometrical rules based on morphological operators to define the final infarcted area. This section provides detailed description of the method, describing it step by step.

Fig. 1. Block scheme of the scar segmentation method

2.1 Pre-processing

The preprocessing step is divided in two parts. On the one hand, some of the myocardial segmentations provided by the STACOM-DEMRI challenge have small segmentation errors. Typically, these consist of: single pixels that are not inside the myocardium but that are marked as such (islands), or pixels inside the myocardium not included in the mask (holes). This is a necessary step for the seed selection and posterior region growing. On the other hand, we have also performed a pre-processing to the DE-MRI slices consisting on an enhancement method to improve the contrast: we have applied a sigmoid function to the gray levels of the image (see Fig. 2).

2.2 Automatic Seed Selection

After the pre-processing step, we proceed to automatically select the seeds that will be used for the region growing algorithm: two seeds at most for scar tissue

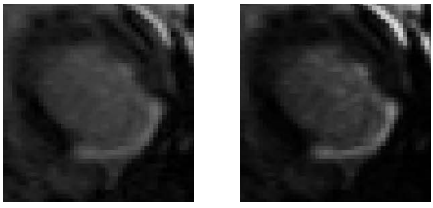

Fig. 2. Application of sigmoid function: original (left) and processed image (right)

and two at most for healthy tissue. To do so, we consider as scar candidates any pixel v_i in slice i with coordinates (x, y) if:

$$v_i(x, y) \text{ is "scar candidate" if } v_i(x, y) > \mu_i + 2\sigma_i, \quad (1)$$

where μ is the mean gray level value of the myocardium and σ is the standard deviation of the gray levels inside the myocardium in the slice that is being analyzed. This gives us a first approximation of possible locations of scar (Fig. 3a). We discard as scar candidates very thin and elongated regions which are near the epicardium, as they often come from errors in the segmentation of the myocardium. We choose the brightest pixels in the one or two bigger regions (single pixels or small islands are discarded) as seeds for scar region growing, and the darkest pixels in the myocardium which are outside the preliminary scar zone and which are inside connected big regions as seeds for the healthy region growing, as depicted in Fig. 3b. With the selected seeds, our method has then from one to four seeds to grow, depending on whether it found no scar, one scar and one healthy region, two scar regions and one healthy or two scar regions and two healthy regions. The possible use of two seeds for scar, instead of just one, solves the problem of having two disconnected regions.

2.3 Region Growing

Region growing is a pixel-based image segmentation method. A region is iteratively grown by comparing all unallocated neighboring pixels to the region [17]. Starting with the seeds chosen as explained in Sec. 2.2, we apply the region growing algorithm, which takes pixels and compares them with its neighbors using an intensity distance related to the standard deviation.

The region growing is performed independently for every seed (the scar ones and healthy). During this step, we do not control if regions overlap or not, the region iteratively grows by comparing all unallocated neighboring pixels to the region. The difference between a pixel intensity value and the region mean is used as a measure of similarity. The pixel with the smallest difference is allocated to the respective region. The process grows the region until the stopping criteria

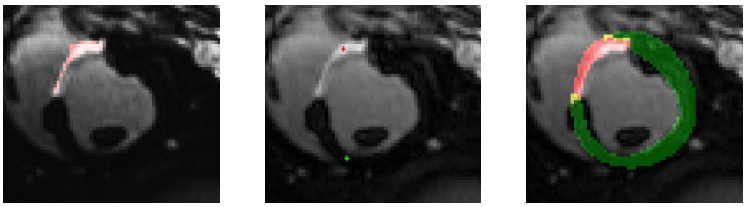

(a) (b) (c)

Fig. 3. Evolution of the algorithm: (a) shows the candidate pixels for scar seeds, (b) shows the seeds for scar tissue (red dot) and healthy tissue (green dot) and (c) shows the three labels: red for "scar", green for "healthy" and yellow for "other"

is met. The regions will, in most of the cases, overlap in some parts of the myocardium. Also, in some cases, some parts of the myocardium are not included neither in the healthy regions nor in the scar ones.

2.4 Region Labeling

Once the region growing algorithm has defined the (possibly overlapping) healthy and scar regions, we proceed to label each pixel as "scar", "healthy" or "other", where "other" could include border-zone and segmentation errors. The labeling uses the following rules:

$$\begin{cases} v_i(x,y) \text{ is "scar"} & \text{if} \quad v_i(x,y) \in R_s \ \& \ \notin R_h, \\ v_i(x,y) \text{ is "healthy"} & \text{if} \quad v_i(x,y) \notin R_s \ \& \ \in R_h, \\ v_i(x,y) \text{ is "other"} & \text{if} \quad \text{otherwise}, \end{cases} \tag{2}$$

where R_s are the scar regions and R_h are the healthy regions. As can be seen from above expressions, we label as "scar" any pixel which is included only in the scar regions. Similarly, "healthy" label is assigned to every pixel which is only included in the "healthy" regions. Any other pixel (included both in healthy and scar regions or not included in any region) is labeled as "other".

A second labeling step is performed for the tissue labeled in the previous step as "other":

$$\begin{cases} v_i(x,y) \in \text{"other" is "scar"} & \text{if} \quad v_i(x,y) \text{ neighbor with "scar"}, \\ v_i(x,y) \in \text{"other" is "other"} & \text{if} \quad \text{otherwise}, \end{cases} \tag{3}$$

where we consider as part of the scar tissue labeled as "other" which is in contact with "scar".

This gives us a myocardium with three labels, "scar" for pixels considered as scar, "healthy" for pixels considered as healthy tissue, and "other" for pixels that are either viable ischemic tissue or miss-segmentations, as shown in Fig. 3c.

2.5 Post-processing

Once we have the labeling, we want to fill the small holes so that there are no isolated pixels in any region. We perform the hole filling both for the regions labeled as "scar" and for the regions labeled as "healthy". Also, we exclude from scar all regions that are too small proportional to the area of the myocardium, which often come from noise in the acquisition, and the connected regions, which were not considered very small but that are attached to the epicardial or endocardial contours and that are very thin and elongated, considering them segmentation errors. Finally, we relabel as scar some patchy, dark regions without contrast which are fully surrounded by enhanced regions, which are consistent with microvascular obstruction and thus should belong to the infarct (see Fig. 5).

Table 1. DSC between automatic and manual segmentations

	1	2	3	4	5	Average
PIGS	0.6739	0.6072	0.8164	0.8615	0.8070	0.7532
HUMANS	0.4400	0.5600	0.6395	0.4048	0.6703	0.5429

3 Results

The STACOM-DEMRI Challenge dataset consists of 30 DE-MRI volumes for segmentation of enhanced regions from post-myocardial infarction patients (15) and pigs (15) that have been subjected to myocardial ischaemia. However, only 5 pigs and 5 humans are provided as training samples with manual annotations for the scar and these 10 volumes have been used to validate our method.

Validation of the method is done by comparing the automatic segmentation results with the manual ones from one observer by calculating the Dice similarity coefficient (DSC) (measuring the degree of area overlap). DSC is always between 0 and 1, with higher DSC indicating better match between automatic and manual segmentations. DSC is 0 for situations in which one of the segmentations shows scar and the other does not, and it is 1 when there is perfect agreement in the segmentations, including the cases where both segmentations show no scar. Table 1 shows the average DSC of each subject.

Figs. 4 and 5 show some visual results for scar segmentation, both for pigs and humans. In the figures, we can compare manual segmentation (top row) with our segmentation (bottom row). The DSC value between the automatically identified and manually defined regions are also shown below each slice. The first two columns of Fig. 4 show cases that have properly worked, the borders

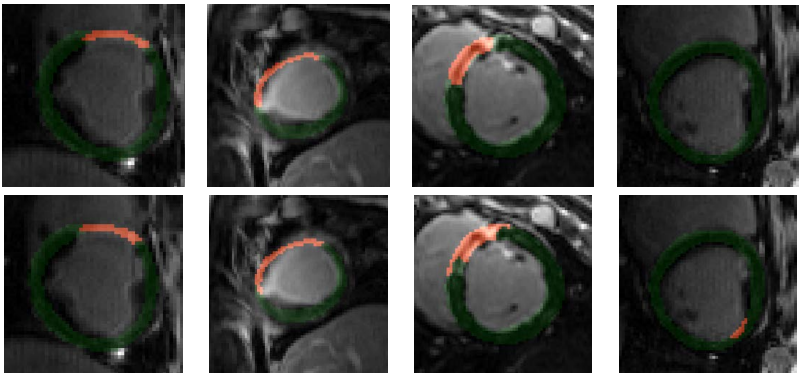

Fig. 4. Examples of our proposed scar location approach (bottom) compared with the manual ground truth (top) for the pig dataset and its DSC value

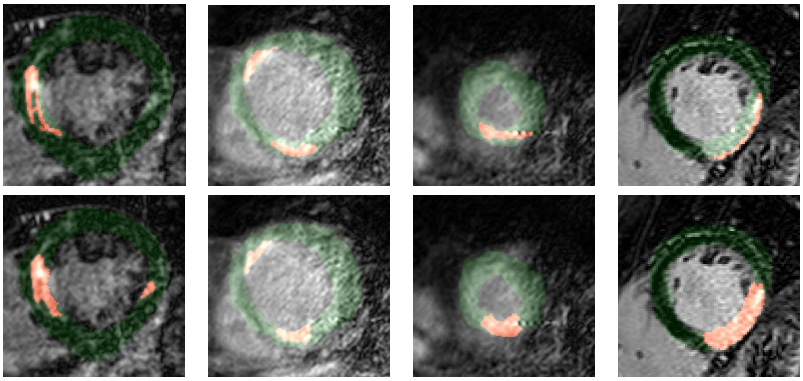

Fig. 5. Examples of our proposed scar location approach (bottom) compared with the manual ground truth (top) for the human dataset and its DSC value

of the scar have been accurately defined. The third column shows a case where the segmentation could have errors due to lack of penetration, but it performs quite well thanks to the double seed initialization and the hole filling. It can be noticed that the DSC is sensitive to the scar size observing the first three values of the measure. Finally, the fourth column of Fig. 4 depicts an error that comes from a bad segmentation of the myocardium, which makes our algorithm fail and detect as scar tissue next to the myocardium.

Fig. 5 shows some segmentations performed on the human dataset. The first column shows a case with correct scar detection, filling the holes without contrast inside the scar that come probably from microvascular obstruction, even though the ground truth provided does not consider these holes as scar. The second column shows an example of double scar detection thanks to the use of two scar and two healthy tissue seeds. The third column shows a typical example of the segmentations being affected by a low contrast and acquisition artifacts. Finally, the fourth column gives a clear example of false positive scar detection due to incorrect myocardial segmentation: a large amount of what seems to be blood pool has been included in the myocardium, and our algorithm has annotated this region, which is exactly next to the real scar, as scar.

Our algorithm is fast enough to be used in real time: the average computational time for one slice is between 0.1 and 4 seconds (depending on the resolution and if any scar seed is detected) when executed in Matlab in a Intel(R) Core(TM)2 Quad CPI Q6600 @ 2.40GHz with windows 7. This makes it usable in clinical scenarios, especially if we consider the fact that the code can be further optimized and refined.

4 Conclusions

We have presented a fully automatic method to segment scar in DE-MRI images. This method has three characteristics that make it very interesting for clinical

practice: it does not require training, it can be used in real time and includes three types of tissue in the labeling: "scar", "healthy" and "other", which includes both possible areas of ischemic viable tissue and voxels that are not really myocardium but were included probably due to segmentation errors.

Our segmentation method is fast enough to be used in real time in a clinical scenario. The most time consuming step of the processing would be the manual segmentation of the myocardium. Using a fast automatic myocardial segmentation, such as the one presented in [5], would help to improve this.

Segmentation results using this method look promising. False positives often come from myocardial segmentation errors. Also, we would like to point out that often, when performing an undersegmentation of a scar, the undersegmented voxels are labeled as "other" and not as healthy. This is important because it indicates to the clinicians that in this area we do not consider the tissue as fully healthy, and that it should be analyzed with caution. Further analysis and evaluation of the performance of this method with a larger dataset has to be performed in order to test its full potential.

References

[1] Vogel-Claussen, J., Rochitte, C., Wu, K.C., Kamel, I.R., Foo, T.K., Lima, J.A.C., Bluemke, D.: Delayed enhancement MR imaging: Utility in myocardial assessment. RadioGraphics 26, 795–810 (2006)

[2] Kim, R.J., Fieno, D.S., Parrish, T.B., Harris, K., Chen, E., Simonetti, O., Bundy, J., Finn, J.P., Klocke, F.J., Judd, R.M.: Relationship of MRI delayed contrast enhancement to irreversible injury, infarct age, and contractile function. Circulation 100, 1992–2002 (1999)

[3] Dikici, E., O'Donnell, T., Setser, R., White, R.D.: Quantification of Delayed Enhancement MR Images. In: Barillot, C., Haynor, D.R., Hellier, P. (eds.) MICCAI 2004. LNCS, vol. 3216, pp. 250–257. Springer, Heidelberg (2004)

[4] Berbari, R.E., Kachenoura, N., Frouin, F., Herment, A., Mousseaux, E., Bloch, I.: An automated quantification of the transmural myocardial infarct extent using cardiac DE-MR images. In: Proc. Int. Conf. IEEE Engineering in Medicine and Biology Society (EMBS) (2009)

[5] Albà, X., Figueras i Ventura, R., Lekadir, K., Frangi, A.F.: Conical deformable model for myocardial segmentation in late-enhanced MRI. In: IEEE International Symposium on Biomedical Imaging (ISBI) (2012)

[6] Heiberg, E., Engblom, H., Engvall, J., Hedström, E., Ugander, M., Arheden, H.: Semi-automatic quantification of myocardial infarction from delayed contrast enhanced magnetic resonance imaging. Scandinavian Cardiovascular Journal 39, 267–275 (2005)

[7] Breeuwer, M., Paetsch, I., Nagel, E., Muthupillai, R., Flamm, S., Plein, S., Ridgway, J.: The detection of normal, ischemic and infarcted myocardial tissue using MRI. Computer Assisted Radiology and Surgery 1256, 1153–1158 (2003)

[8] Kolipaka, A., Chatzimavroudis, G.P., White, R.D., O'Donnell, T.P., Setser, R.M.: Segmentation of non-viable myocardium in delayed enhancement magnetic resonance images. International Journal of Cardiovascular Imaging 21, 303–311 (2005)

[9] Positano, V., Pingitore, A., Giorgetti, A., Favilli, B., Santarelli, M., Landini, L., Marzullo, P., Lombardi, M.: A fast and effective method to assess myocardial necrosis by means of contrast magnetic resonance imaging. Journal of Cardiovascular Magnetic Resonance 7, 487–494 (2005)
[10] O'Donnell, T.P., Xu, N., Setser, R.M., White, R.D.: Semi-automatic segmentation of nonviable cardiac tissue using cine and delayed enhancement magnetic resonance images. In: Proc. SPIE Medical Imaging, vol. 5031, pp. 242–251 (2003)
[11] Hsu, L.Y., Natanzon, A., Kellman, P., Hirsch, G.A., Aletras, A.H., Arai, A.E.: Quantitative myocardial infarction on delayed enhancement MRI. Part I: animal validation of an automated feature analysis and combined thresholding infarct sizing algorithm. Journal Magnetic Resonance Imaging 23, 298–308 (2006)
[12] Tao, Q., Milles, J., Zeppenfeld, K., Lamb, H.J., Bax, J.J., Reiber, J.H., van der Geest, R.J.: Automated segmentation of myocardial scar in late enhancement MRI using combined intensity and spatial information. Magnetic Resonance in Medicine 64, 586–594 (2010)
[13] Kachenoura, N., Redheuil, A., Herment, A., Mousseaux, E., Frouin, F.: Robust assessment of the transmural extent of myocardial infarction in late gadolinium-enhanced MRI studies using appropriate angular and circumferential subdivision of the myocardium. European Radiology 18, 2140–2147 (2008)
[14] Hennemuth, A., Seeger, A., Friman, O., Miller, S., Klumpp, B., Oeltze, S., Peitgen, H.: A comprehensive approach to the analysis of contrast enhanced cardiac MR images. IEEE Transactions on Medical Imaging 27, 1592–1610 (2008)
[15] Elagouni, K., Ciofolo-Veit, C., Mory, B.: Automatic segmentation of pathological tissues in cardiac MRI. In: IEEE International Symposium on Biomedical Imaging (ISBI), pp. 472–475 (2010)
[16] Elnakib, A., Beache, G.M., Nitzken, M., Gimel'jarb, G., EI-Baz, A.: A new framework for automated identification of pathological tissues in contrast enhanced cardiac magnetic resonance images. In: IEEE International Symposium on Biomedical Imaging (ISBI), pp. 1272–1275 (2011)
[17] Adams, R., Bischof, L.: Seeded region growing. IEEE Transactions on Pattern Analysis and Machine Intelligence 16(6), 641–647 (1994)